

Ferromagnetic Coupling between Low- and High-Spin Iron(III) Ions in the Tetranuclear Complex $fac\{-[Fe^{III}\{HB(pz)_3\}(CN)_2(\mu-CN)_3]Fe^{III}(H_2O)_3\}\cdot 6H_2O$ ($[HB(pz)_3]^- = \text{Hydrotris(1-pyrazolyl)borate}$)

Rodrigue Lescouëzec,^{1a} Jacqueline Vaissermann,^{1b} Francesc Lloret,^{1a} Miguel Julve,^{*1a} and Michel Verdaguer^{*1b}

Departament de Química Inorgànica/Instituto de Ciencia Molecular, Facultat de Química de la Universitat de València, Dr. Moliner 50, 46100-Burjassot, València, Spain, and Laboratoire de Chimie Inorganique et Matériaux Moléculaires, Unité CNRS 7071, Université Pierre et Marie Curie, 4 Place Jussieu, Case 42, 75252 Paris Cedex 05, France

Received May 29, 2002

The novel mononuclear $PPh_4\text{-}fac\text{-}[Fe^{III}\{HB(pz)_3\}(CN)_3]\cdot H_2O$ (**1**) [PPh_4^+ = tetraphenylphosphonium cation; $(HB(pz)_3)^-$ = hydrotris(1-pyrazolyl)borate] and tetranuclear $fac\{-[Fe^{III}\{HB(pz)_3\}(CN)_2(\mu-CN)_3]Fe^{III}(H_2O)_3\}\cdot 6H_2O$ (**2**) have been prepared and characterized by X-ray diffraction analysis. Crystal data for compound **1**: monoclinic, space group $P2_1/c$, $a = 9.575(3)$ Å, $b = 21.984(4)$ Å, $c = 16.863(3)$ Å, $\beta = 100.34(2)^\circ$, $U = 3486(1)$ Å³, $Z = 4$. Crystal data for compound **2**: orthorhombic, space group $Pnam$, $a = 14.084(3)$ Å, $b = 14.799(4)$ Å, $c = 25.725(5)$ Å, $U = 5362(2)$ Å³, $Z = 4$. Compound **1** is a low-spin iron(III) compound with three cyanide ligands in *fac* arrangement and a tridentate pyrazolylborate ligand building a distorted octahedral environment around the iron atom. Compound **2** is the first example of a molecular species containing three peripheral low-spin iron(III) ions linked to a central high-spin iron(III) cation by single cyanide bridges, the anion of **1** acting as a monodentate ligand in **2**. Variable-temperature magnetic susceptibility measurements of **2** reveal the occurrence of a significant ferromagnetic coupling between the three peripheral low-spin iron(III) centers and the central high-spin iron(III) ion cations leading to a low-lying nonet spin state.

Some exciting results were obtained recently in the old family of Prussian blue analogues: the achievement of molecule-based magnets with critical temperatures (T_c 's) as high as 376^{2,3} and photoinduced magnetization.^{4,5} These three-dimensional compounds are easily obtained as powder samples by reaction of the hexacyanometalate unit $[B(CN)_6]^{q-}$ with the totally hydrated metal ions $[A(H_2O)_6]^{p+}$ (A and B are transition metal ions). Their exciting photomagnetic properties and the usefulness of lower nuclearity models to interpret their properties prompted experimental chemists to

look for different synthetic strategies by modifying the bonding ability of Lewis acid A or/and Lewis base B.^{6–12} Three recent examples based on the modification of the B unit are the following: (i) the 14-metal $[(Me_3tacn)_8Cr_8Ni_6(CN)_{24}]^{12+}$ and 19-metal $[(Me_3tacn)_{10}Cr_{10}Ni_9(CN)_{42}]^{6+}$ assemblies ($Me_3tacn = N,N',N''$ -trimethyl-1,4,7-triazacyclononane) obtained by using the neutral *fac*- $[Cr(Me_3tacn)_3(CN)_3]$ complex as cyanide precursor;^{10a} (ii) the cyclic tetranuclear complex $[Fe^{III}_2(bipy)_4(CN)_4Cu^{II}_2(bipy)_2]^{6+}$ ($bipy = 2,2'$ -bipyridine) which exhibits a quintet spin ground state, where the B unit is the dicyano low-spin iron(III) complex $[Fe(bipy)_2(CN)_2]^+$;¹¹ (iii) the trinuclear complexes *trans*- $[Fe^{III}(bipy)(CN)_4]_2M^{II}(H_2O)_4\cdot 4H_2O$ and the double zigzag chains $[Fe^{III}(phen)(CN)_4]_2M^{II}(H_2O)_2\cdot 4H_2O$ ($M = Mn$ and Zn ; $phen = 1,10$ -phenanthroline) with antiferromagnetic

- (4) (a) Shimamoto, N.; Ohkoshi, S. I.; Sato, O.; Hashimoto, K. *Inorg. Chem.* **2002**, *41*, 678. (b) Sato, O.; Einaga, A.; Fujishima, A.; Hashimoto, K. *Inorg. Chem.* **1999**, *38*, 4405. (c) Sato, O.; Iyoda, T.; Fujishima, A.; Hashimoto, K. *Science* **1996**, *271*, 49.
- (5) (a) Bleuzen, A.; Lomenech, C.; Escax, V.; Villain, F.; Varret, F.; Cartier dit Moulin, C.; Verdaguer, M. *J. Am. Chem. Soc.* **2000**, *122*, 6648. (b) Cartier dit Moulin, C.; Villain, F.; Bleuzen, A.; Arrio, M. A.; Sainctavit, P.; Lomenech, C.; Escax, V.; Baudelet, F.; Dartyge, E.; Gallet, J. J.; Verdaguer, M. *J. Am. Chem. Soc.* **2000**, *122*, 6653. (c) Escax, V.; Bleuzen, A.; Verdaguer, M.; Cartier dit Moulin, C.; Villain, F. *J. Am. Chem. Soc.* **2001**, *123*, 12536. (d) Champion, G.; Cartier dit Moulin, C.; Villain, F.; Bleuzen, A.; Baudelet, F.; Dartyge, E.; Verdaguer, M. *J. Am. Chem. Soc.* **2001**, *123*, 12544.
- (6) Ohba, M.; Okawa, H. *Coord. Chem. Rev.* **2000**, *198*, 313 and references therein.
- (7) Mallah, T.; Marvilliers, A.; Rivière, E. *Philos. Trans. R. Soc. London, Ser. A* **1999**, *357*, 3139.
- (8) Parker, R. J.; Spiccia, L.; Batten, S. R.; Cashion, J. D.; Fallon, G. D. *Inorg. Chem.* **2001**, *40*, 4696.
- (9) (a) Smith, J. A.; Galán-Mascarós, J. R.; Clérac, R.; Sun, J. S.; Ouyang, X.; Dunbar, K. R. *Polyhedron* **2001**, *20*, 1727. (b) Smith, J. A.; Galán-Mascarós, J. R.; Clérac, R.; Dunbar, K. R. *Chem. Commun.* **2000**, 1077.
- (10) (a) Sokol, J. J.; Shores, M. P.; Long, J. R. *Angew. Chem., Int. Ed.* **2001**, *40*, 236. (b) Berseth, P. A.; Sokol, J. J.; Shores, M. P.; Heinrich, J. L.; Long, J. R. *J. Am. Chem. Soc.* **2000**, *122*, 9655. (c) Heinrich, J. L.; Berseth, P. A.; Long, J. R. *Chem. Commun.* **1997**, 1231.
- (11) Oshio, H.; Tamada, O.; Onodera, H.; Ito, T.; Ikoma, T.; Tero-Kubota, S. *Inorg. Chem.* **1999**, *38*, 5686.
- (12) (a) Lescouëzec, R.; Lloret, F.; Julve, M.; Vaissermann, J.; Verdaguer, M. *Inorg. Chem.* **2002**, *41*, 818. (b) Lescouëzec, R.; Lloret, F.; Julve, M.; Vaissermann, J.; Verdaguer, M.; Llusar, R.; Uriel, S. *Inorg. Chem.* **2001**, *40*, 2065.

* To whom correspondence should be addressed. E-mail: miguel.julve@uv.es (M.J.); miv@ccr.jussieu.fr (M.V.).

(1) (a) Universitat de València. (b) Université Pierre et Marie Curie.
 (2) Holmes, S. M.; Girolami, G. *J. Am. Chem. Soc.* **1999**, *121*, 5593.
 (3) Ferlay, S.; Mallah, T.; Ouahès, R.; Veillet, P.; Verdaguer, M. *Nature* **1995**, *378*, 701.

COMMUNICATION

coupling between Fe(III) and Mn(II), where the B unit is the tetracyano low-spin iron(III) complex $[\text{Fe}(\text{L})(\text{CN})_4]^-$ ($\text{L} = \text{bipy}$ and phen).¹²

In our efforts to design novel cyanometalate precursors, we prepared the mononuclear complex $\text{PPh}_4\text{-fac-}[\text{Fe}\{\text{HB}(\text{pz})_3\}(\text{CN})_3]\cdot\text{H}_2\text{O}$ (**1**) [PPh_4^+ = tetraphenylphosphonium cation; $[\text{HB}(\text{pz})_3]^-$ = hydrotris(1-pyrazolyl)borate] and the tetranuclear compound $\text{fac-}\{[\text{Fe}^{\text{III}}\{\text{HB}(\text{pz})_3\}(\text{CN})_2(\mu\text{-CN})]_3\text{Fe}^{\text{III}}(\text{H}_2\text{O})_3\}\cdot 6\text{H}_2\text{O}$ (**2**) obtained by reaction between the anion of **1** and $[\text{Fe}(\text{H}_2\text{O})_6]^{3+}$ in water.¹³ Both compounds were characterized by IR spectroscopy, variable-temperature magnetic measurements,¹⁴ and X-ray structural analysis.¹⁵

The crystal structure of **1** consists of $\text{fac-}[\text{Fe}\{\text{HB}(\text{pz})_3\}(\text{CN})_3]^-$ anions (see Figure 1), uncoordinated tetraphenylphosphonium cations, and crystallization water molecules. The iron atom has a slightly distorted octahedral coordination geometry, its symmetry being close to C_{3v} . The distances between the iron and the nitrogens of the pyrazolylborate ligand vary in the range 1.970(4)–1.987(4) Å, considerably shorter than those found in the high-spin iron(III) complex $\{\text{Fe}[\text{HB}(\text{pz})_3]\text{Cl}_3\}^-$ [2.152(4)–2.175(5) Å]¹⁹ and close to those reported for the low-spin iron(II) compound $\{\text{Fe}[\text{HB}(\text{pz})_3]_2\}$ (1.96–1.98 Å).²⁰ Good agreement is observed between the Fe(1)–C(cyano) bond distances of **1** [1.910(6)–1.929(7) Å] and those reported for other cyano-containing mononuclear low-spin iron(III) [1.87(2)–1.95(1) Å]^{12,21} and iron(II) [1.891(5)–1.936(5) Å]²² complexes. The presence of the tetraphenylphosphonium cation in the structure of **1**, the value of the magnetic moment at room temperature (μ_{eff} ca. 2.4 μ_B), and the cyanide stretching frequency [ca. 2123s

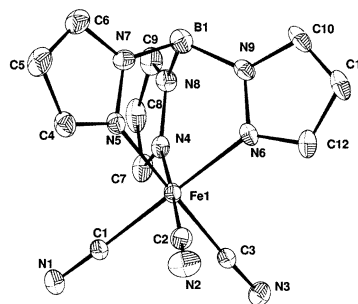


Figure 1. Perspective view of the anion of **1** showing the atom numbering (thermal ellipsoids for 30% probability). Hydrogen atoms are omitted. Selected bond lengths [Å] and angles [deg]: Fe(1)–C(1), 1.910(6); Fe(1)–C(2), 1.929(7); Fe(1)–C(3), 1.917(5); Fe(1)–N(4), 1.970(4); Fe(1)–N(5), 1.987(4); Fe(1)–N(6), 1.984(4); C(1)–Fe(1)–C(2), 86.7(3); C(1)–Fe(1)–N(4), 91.7(2); C(1)–Fe(1)–N(6), 179.3(2); C(1)–Fe(1)–C(3), 87.1(2); C(1)–Fe(1)–N(5), 92.8(2); C(2)–Fe(1)–N(6), 92.6(2); C(2)–Fe(1)–N(4), 178.2(2); C(2)–Fe(1)–C(3), 90.9(2); C(2)–Fe(1)–N(5), 91.8(2); N(4)–Fe(1)–N(6), 89.0(2); N(4)–Fe(1)–C(3), 90.0(2); N(4)–Fe(1)–N(5), 87.3(2); N(6)–Fe(1)–C(3), 93.1(2); N(6)–Fe(1)–N(5), 86.9(2); C(3)–Fe(1)–N(5), 177.3(2).

cm^{-1} in **1** versus 2118s and 2120s cm^{-1} for the low-spin iron(III) complexes $\text{PPh}_4[\text{Fe}(\text{L})(\text{CN})_4]\cdot n\text{H}_2\text{O}$ with $\text{L} = \text{bipy}$ ($n = 1$) and phen ($n = 2$)¹² unambiguously reveal a low-spin iron(III) species. The PPh_4^+ cations are grouped by pairs exhibiting the edge-to-face interaction pattern with a $\text{P}\cdots\text{P}$ separation of 6.575(3) Å²³ (see Figure S1 in the Supporting Information). The anions are linked through hydrogen bonds involving the uncoordinated water molecule [O(1)] and two

- (13) $\text{PPh}_4\{[\text{Fe}\{\text{HB}(\text{pz})_3\}(\text{CN})_3]\cdot\text{H}_2\text{O}$ (**1**): $\{\text{Fe}^{\text{II}}[\text{HB}(\text{pz})_3]_2\}$ (1.93 g, 4 mmol) and PPh_4CN (4.38 g, 12 mmol) were mixed in 2-propanol (50 mL), and the resulting suspension was heated at 80 °C for 90 min under continuous stirring. The initial purple solid which turned yellowish brown was filtered off, washed with hot water, and air-dried. It was dissolved in a chloroform/2-propanol (4:1) mixture, the small fraction of insoluble material (unreacted $\{\text{Fe}^{\text{II}}[\text{HB}(\text{pz})_3]_2\}$) being removed by filtration. Dropwise addition of 30% H_2O_2 to this solution causes the precipitation of **1** as a yellow crystalline solid. An additional crop of **1** is obtained by slow evaporation of the solution at room temperature. Crystals of **1** as yellow parallelepipeds suitable for X-ray diffraction were grown by recrystallization of the yellow solid in a MeCN/ H_2O (9:1) mixture. The yield is ca. 70% (on the basis of the starting iron salt). The temperature and the heating time are critical parameters in the preparation of **1** because it undergoes decomposition when overheated. The use of KCN instead of PPh_4CN allows us to prepare $\text{K}\{[\text{Fe}\{\text{HB}(\text{pz})_3\}(\text{CN})_3]\cdot 2\text{H}_2\text{O}$ by following the same procedure but heating 12 h. The yield is practically the same as that of **1**. Anal. (%) Calcd for $\text{C}_{36}\text{H}_{32}\text{BF}_4\text{FeN}_9\text{O}$ (**1**): C, 61.42; H, 4.55; N, 17.90. Found: C, 61.08; H, 4.44; N, 17.79. IR stretching cyanide/ cm^{-1} : 2123s (**1**). $\text{fac-}\{[\text{Fe}^{\text{III}}\{\text{HB}(\text{pz})_3\}(\text{CN})_2(\mu\text{-CN})]_3\text{Fe}^{\text{III}}(\text{H}_2\text{O})_3\}\cdot 6\text{H}_2\text{O}$ (**2**): $\text{Fe}(\text{NO}_3)_3\cdot 9\text{H}_2\text{O}$ (40 mg, 0.1 mmol) dissolved in a small volume of water (5 mL) is added to an aqueous solution (30 mL) of $\text{K}\{[\text{Fe}\{\text{HB}(\text{pz})_3\}(\text{CN})_3]\cdot 2\text{H}_2\text{O}$ (127 mg, 0.3 mmol). Red rodlike crystals of **2** suitable for X-ray analysis separated from the resulting deep red solution on standing at room temperature after 1 day. Several crops of crystals of **2** were collected by slow evaporation and dried on filter paper. An orange precipitate of iron(III) oxide is also formed and daily removed. The yield of **2** is ca. 50% (based on the iron(III) nitrate). Anal. (%) Calcd for $\text{C}_{36}\text{H}_{48}\text{B}_3\text{Fe}_4\text{N}_{27}\text{O}_9$ (**2**): C, 34.36; H, 3.82; N, 30.04. Found: C, 34.12; H, 3.75; N, 29.85. IR stretching cyanide/ cm^{-1} : 2154m and 2134s (**2**).

- (14) Magnetic susceptibility data were collected on polycrystalline samples with a Quantum Design SQUID magnetometer in the temperature range 1.9–290 K (**2**) and at 290 K (**1**) under an applied magnetic field of 1.5 T (above 50 K) and 0.25 T (below 50 K) to avoid saturation effects. The magnetic data were corrected for diamagnetism of the constituent atoms estimated from Pascal's constants.

- (15) Crystallographic analyses for **1** ($\text{C}_{36}\text{H}_{32}\text{BF}_4\text{FeN}_9\text{O}$): $T = 295$ K, monoclinic, space group $P2_1/c$, $a = 9.575(3)$ Å, $b = 21.984(4)$ Å, $c = 16.863(3)$ Å, $\beta = 100.34(2)^\circ$, $U = 3486(1)$ Å³, $Z = 4$, $\rho_{\text{calcd}} = 1.34$ g cm^{-3} , $\mu = 5.18$ cm^{-1} , $R1 = 0.046$, $wR2 = 0.054$ for 2785 observed reflections with $I > 3\sigma(I)$ (from the 6705 collected in the θ range 1–25°, 6118 were unique), 443 parameters, residual maximum and minimum in the final Fourier difference maps were 0.60 and -0.31 e Å⁻³. For **2** ($\text{C}_{36}\text{H}_{48}\text{B}_3\text{Fe}_4\text{N}_{27}\text{O}_9$): $T = 295$ K, orthorhombic, space group $Pnam$, $a = 14.084(3)$ Å, $b = 14.799(4)$ Å, $c = 25.725(5)$ Å, $U = 5362(2)$ Å³, $Z = 4$, $\rho_{\text{calcd}} = 1.56$ g cm^{-3} , $\mu = 11.3$ cm^{-1} , $R1 = 0.0548$, $wR2 = 0.0646$ for 1651 observed reflections with $I > 3\sigma(I)$ (from the 5255 collected in the θ range 1–25°, 4829 were unique), 173 parameters, residual maximum and minimum in the final Fourier difference maps were 0.65 and -0.56 e Å⁻³. Diffraction data of **1** and **2** were collected on an Enraf-Nonius CAD-4 diffractometer using graphite-monochromated Mo K α radiation ($\lambda = 0.71069$ Å) and were corrected for Lorentz and polarization effects. An empirical absorption correction was performed by the use of DIFABS¹⁶ (**1**) and the Ψ -scan curve (**2**). The structures of **1** and **2** were solved by direct methods through SHELX-86¹⁷ and subsequently refined by Fourier recycling. The final full-matrix least-squares refinement on F was done by the PC version of CRYSTALS.¹⁸ All non-hydrogen atoms of **1** were refined anisotropically whereas those of **2** were isotropically refined. All hydrogen atoms (except those of the boron atoms in **2** which were found on a difference Fourier map) were introduced in calculated positions and were allocated one overall isotropic thermal parameter.

- (16) Walker, N.; Stuart, D. *Acta Crystallogr.* **1983**, A39, 156.
 (17) (a) Sheldrick, G. M. *SHELX-86: Program for Crystal Structure Solution*; University of Göttingen: Göttingen, Germany, 1996. (b) Watkin, D. J.; Prout, C. K.; Pearce, L. J. *CAMERON*; Crystallography Laboratory, University of Oxford: Oxford, U.K., 1996.
 (18) Watkin, D. J.; Prout, C. K.; Carruthers, J. R.; Betteridge, P. W. *CRYSTALS*; Chemical Crystallography Laboratory, University of Oxford: Oxford, U.K., 1996; Issue 10.
 (19) Fukui, H.; Ito, M.; Moro-oka, Y.; Kitajima, N. *Inorg. Chem.* **1990**, 29, 2868.
 (20) Oliver, J. D.; Mullica, D. F.; Hutchinson, B. B.; Milligan, W. O. *Inorg. Chem.* **1980**, 19, 165.
 (21) Lu, T. H.; Kao, H. Y.; Wu, D. I.; Kong, K. C.; Cheng, C. H. *Acta Crystallogr.* **1988**, C44, 1184.
 (22) (a) Nieuwenhuyzen, M.; Bertram, B.; Gallagher, J. F.; Vos, J. G. *Acta Crystallogr.* **1988**, C54, 603. (b) Zhan, S.; Meng, Q.; You, X.; Wang, G.; Zheng, P. *J. Polyhedron* **1996**, 15, 2665.

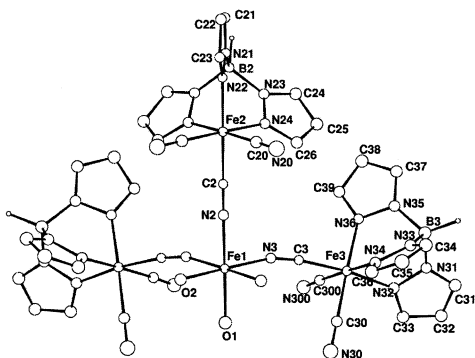


Figure 2. Perspective view of the tetranuclear unit of **2** showing the atom numbering. Selected bond lengths [Å] and angles [deg]: Fe(1)–O(1), 1.99(1); Fe(1)–O(2), 2.030(8); Fe(1)–N(2), 2.02(1); Fe(1)–N(3), 2.049(8); O(1)–Fe(1)–O(2), 88.7(3); O(1)–Fe(1)–N(2), 173.9(5); O(1)–Fe(1)–N(3), 91.2(3); O(2)–Fe(1)–O(2'), 89.4(4); O(2)–Fe(1)–N(3'), 88.1(3); O(2)–Fe(1)–N(3), 177.4(3); O(2)–Fe(1)–N(2), 87.0(3); N(3)–Fe(1)–N(3'), 94.5(5); N(2)–Fe(1)–N(3), 92.9(3); Fe(1)–N(2)–C(2), 173.3(12); Fe(1)–N(3)–C(3), 164.2(8); Fe(2)–C(2)–N(2), 177.7(13); Fe(3)–C(3)–N(3), 171.6(9) [symmetry code: (') = $x, y, 3/2 - z$].

of the three cyanide nitrogens [N(2) and N(3)] [2.886(8) and 2.990(7) Å for O(1)⋯N(2') and O(1)⋯N(3), respectively; (') = $1 - x, y, z$], building a chain of hydrogen bonds which runs parallel to the *a* axis (see Figure S2).

The structure of complex **2** is made up of neutral *fac*-{[Fe^{III}{HB(pz)₃}(CN)₂(μ-CN)₃Fe^{III}(H₂O)₃} tetranuclear units (see Figure 2) and crystallization water molecules which are linked through an extensive network of hydrogen bonds involving the coordinated and uncoordinated water molecules [O⋯O distances varying in the range 2.623(24)–2.633(12) Å] and two nitrogen atoms [N(30) and N(300)] of the terminally bound cyanide ligands [N⋯O = 2.633(12) and 2.750(14) Å]. The anion of **1** is also present in **2**, but here, it acts as a monodentate ligand through one of its three cyanide groups toward a *fac*-trianiron(III) entity affording an original tetranuclear compound where three low-spin iron(III) motifs are bound to a central six-coordinated high-spin iron(III) (see the magnetic properties described here). The Fe–C–N angles for both terminal [174.1(5)–178.3(6)° in **1** and 175.4(11)–178.5(12)° in **2**] and bridging [171.6(9)° and 177.7(13)° in **2**] cyanide groups are somewhat bent. The iron–iron distances through the single cyano bridges are 5.047(3) Å [Fe(1)⋯Fe(2)] and 5.012(2) Å [Fe(1)⋯Fe(3)], values which are shorter than the shortest intermolecular metal–metal separation, 7.434(2) Å [Fe(1)⋯Fe(3a); (a) = $-1/2 + x, 1/2 - y, z$].

The temperature dependence of χ_{MT} , where χ_M is the magnetic susceptibility per four iron(III) ions, in the temperature range 225–1.9 K is shown in Figure 3. At room temperature, χ_{MT} is 6.83 cm³ mol⁻¹ K, which is somewhat higher than that expected for a high-spin ($S = 5/2$) and three low-spin ($S = 1/2$) iron(III) ions magnetically isolated. It continuously increases on cooling and reaches a maximum value of 9.40 cm³ mol⁻¹ K at 14 K (slightly weaker than the value expected for an $S = 4$ spin state, $\chi_{MT} = 10$ cm³ mol⁻¹ K with $g = 2.0$) and further decreases to 6.70 cm³

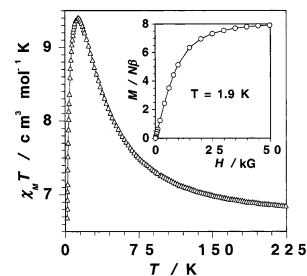


Figure 3. Temperature dependence of the χ_{MT} product for **2**. The inset shows the field dependence of the magnetization of **2** at $T = 1.9$ K [(Δ, ○) experimental data; (—) eye-guide lines].

mol⁻¹ K at 1.9 K. This curve is in agreement with a significant ferromagnetic coupling between the central spin sextuplet and peripheral spin doublets to give a low-lying $S = 4$ spin state. The ferromagnetic nature of this interaction and the nonet ground spin state is evidenced by the magnetization curve at 1.9 K (see inset of Figure 3) which exhibits a saturation value of ca. 8 μ_B at the maximum available magnetic field. Intermolecular interactions and/or zero-field splitting (D) in the $S = 4$ state could account for the decrease of χ_{MT} in the lower temperature region. Alternating current susceptibility measurements, carried out on **2**, in the temperature range 2–10 K do not show the frequency dependence expected for a single-molecule magnet behavior. To evidence such a behavior, if present ($D < 0$ and large enough), lower temperature measurements would be necessary. The large first-order spin–orbit contribution present in the low-spin iron(III) ion (${}^2T_{2g}$ ground term) precludes the analysis of the magnetic properties of **2** through a simple spin Hamiltonian expression. The ferromagnetic interaction in **2** can be understood by taking into account the electronic configuration of the iron and the symmetry of the singly occupied (magnetic) orbitals. The interaction between $t_{2g}^3 e_g^2$ (high-spin iron(III)) and $t_{2g}^5 e_g^0$ (low-spin iron(III)) implies one t_{2g} orbital on the low-spin iron(III) which gives rise to two $t_{2g} - e_g$ ferromagnetic pathways arising from the orthogonality of the orbitals and three $t_{2g} - t_{2g}$ antiferromagnetic pathways associated with the π overlap of the orbitals. Among the three antiferromagnetic pathways, only one is operative [along the Fe(1)–NC–Fe(low-spin) bridges] with an efficiency reduced by the bending of the Fe–NC–Fe bridge. The two ferromagnetic contributions, with an important overlap density on the N(2) and N(3) atoms, can therefore overcome the antiferromagnetic ones. In summary, mononuclear compound **1** is a new suitable building block which allows the preparation of novel discrete high-spin molecules such as **2** and opens wide perspectives in the design of magnetic heterometallic assemblies.

Acknowledgment. This work was supported by the TMR Program from the European Union (Contract ERBFM-RXCT98-0181), the European Science Foundation through the Molecular Magnets Programme, and the Ministerio Español de Ciencia y Tecnología (Project BQU-2001-2928).

Supporting Information Available: Additional figures. Crystallographic data in CIF format. This material is available free of charge via the Internet at <http://pubs.acs.org>.

(23) Dance, I.; Scudder, M. *Chem.–Eur. J.* **1996**, *2*, 481 and references therein.